Effect of Hafnium Carbide Nanoparticles on the Emission Properties of Quasi 2D-Graphene/Nanotube Film: A First Principles Study

© *O.E. Glukhova*[1,2], *M.M. Slepchenkov*[1]

[1] Saratov National Research State University,
Saratov, Russia
[2] I.M. Sechenov First Moscow State Medical University,
Moscow, Russia

E-mail: glukhovaoe@info.sgu.ru

Using computer materials science methods based on first-principles approaches and high-performance computing, we have studied the effect of hafnium carbide (HfC) nanoparticles on the emission properties of graphene/nanotube hybrid films. The optimal distance between graphene/nanotube structures in the composition of the hybrid film and the optimal mass fraction of HfC nanoparticles, which provide the greatest reduction in the electron work function, have been established. It has been found that partial charge transfer from the nanoparticle HfC to the carbon framework leads to changes in the density of electronic states, resulting in a change of both the Fermi energy and the height of the potential barrier for the emitting electron change, which leads to a decrease in the work function of the electron by $8-10\%$.

Keywords: computer materials science, electronic charge distribution, Fermi energy, electron work function, density of electronic states.

1. Introduction

The creation of effective sources of autoelectronic emission for vacuum electronics remains an urgent scientific and technical task for many decades. A new impetus to the development of research in this area was given after the discovery of carbon nanotubes (CNT) [1,2]. Due to the large aspect ratio, high electrical conductivity, thermal and chemical stability, CNT have proven themselves as a promising material for creating field emitters [3–10]. In the future, field emitters made of other carbon nanomaterials, including diamond films, glass carbon and graphene nanostructures, were used in the development of autoemission cathodes [11–15]. In the last decade, hybrid carbon nanostructures formed by graphene and CNT [16–23] have been considered by experts as one of the promising sources of autoelectronic emission. The interest in studying these structures is explained by the synergetic effect arising from the combination of carbon nanostructures of various dimensions (2D-graphene and 1D-nanotubes) and leading to an increase in the mechanical, electronic and optical properties of [24–26]. Prognostic studies of mechanical, electronic, optical and transport properties of hybrid graphene-nanotube structures were carried out using computer modeling methods [27–33]. Promising results have been obtained in the field of theoretical and experimental studies of the emission properties of graphene-nanotube hybrid structures. The results of a first-principle study (*ab initio*) of hybrid structures formed from covalently connected vertically oriented single-walled CNT (SWCNT)

and a graphene sheet are provided in [16]. The results of the calculation by the DFT method (density functional theory) showed that when an external field is applied to the hybrid structure of graphene, a decrease in the band gap is observed. The work function and the ionization potential also decrease with an increase of the field strength, which contributes to the improvement of the auto-emission properties of hybrid graphene structures−SWCNT with vertically oriented nanotubes. The effect of nitrogen atom functionalization on the electronic and emission properties of the hybrid graphene structure−SWCNT with a seamless connection of vertically oriented SWCNT is studied in [17]. Based on the results of DFT calculations, the authors found that for all the variants of nitrogen atom placement considered in the work, it was possible to achieve a significant reduction in the yield and ionization potential of the hybrid graphene structure−SWCNT due to emerging bound electronic states with mixed properties of both localized states and extended states. For hybrid graphene−CNT films experimentally obtained using a method based on low-vacuum annealing of a cellulose acetate solution, emission current densities of $10\,\mu\text{A/cm}^2$ were achieved at an emission inclusion field of $2.12\,\text{V}/\mu\text{m}$ [18]. Using the technology of chemical deposition from the gas phase (CVD) with subsequent heating and cooling allows the synthesis of hybrid films graphene−CNT, demonstrating an emission current density of $1.3\,\text{mA/cm}^2$ with an emission inclusion field of $2.9\,\text{V}/\mu\text{m}$ [19]. The hybrid SWCNT/graphene films produced by electrophoretic deposition showed a significant

emission current of 80 mA with a density of 160 mA/cm^2 with an emission inclusion field of 0.92 V/μm in the mode of pulsed high voltage [23].

As is known, carbon nanomaterials are characterized by a sufficiently large electron yield ($\sim 4.6-4.7$ eV), which forces us to look for ways to effectively functionalize them with other nanostructures with low yield performance. One example of such nanostructures are nanorods, nanowires, nanoparticles and other nanocoating made of hafnium carbide HfC [34–38]. It was experimentally shown in [34] that a single field electron emitter made of HfC nanowire is characterized by the work function of 3.1 eV and demonstrates an emission current of 173 nA at a low pulling voltage of 631 V with an emission gap size of 5 mm. A single HfC nanowire grown on a graphite substrate by the CVD method demonstrated a high field gain — $5.57 \cdot 10^6$ m^{-1}, testifying that a field emitter made on its basis is capable of operating at a lower extraction voltage in a moderately high vacuum [35]. In works [36–38] it was found that the decoration of carbon nanomaterials with hafnium carbide leads to an improvement in their flexibility, thermal and electrical conductivity, as well as the ability to shield electromagnetic waves.

The methods *ab initio* are used in this paper to study 2D-graphene/nanotube films decorated with HfC nanoparticles. The aim of the study is to identify patterns of the influence of the mass fraction of HfC nanoparticles on the electronic and emission properties of carbon films graphene$-$SWCNT.

2. Calculation procedure

The atomistic structure and electronic properties are investigated in this paper using DFT using the generalized gradient approximation (GGA) of Purdue-Burke-Ernzerhoff (PBE), implemented in the SIESTA software package [39,40]. An optimization is performed to obtain the equilibrium configuration of crystal cells (supercells) which consists in solving the minimax problem for identifying the global minimum of total energy by varying the coordinates of all atoms and the lengths of the translation vectors. A basic set of split valence orbitals of the DZP (double zeta polarization) with polarization functions was used. The Monkhorst–Pack scheme was applied to construct a grid of k-points and partition the inverse space [41]. The atomic structure was optimized with an accuracy of 0.04 eV/Å for interatomic forces and with an accuracy of 10^{-5} eV for total energy. The search for the global minimum of total energy was carried out using the Broyden–Pooley [42] scheme. The first Brillouin zone was described by a grid of $10 \times 1 \times 1$ k-points. The cutoff of the real spatial grid in all calculations was chosen to be equal to 600 Ry. The distribution of the electron charge density across atoms was determined in accordance with the orbitals Mulliken population analysis [43]. Grimm's empirical correction [44] was used to correctly account for the van der Waals inter-

action between neighboring graphene/nanotube structures in the film composition. The electron work function was calculated using the formula

$$\Phi = E_{\text{vac}} - E_{\text{F}}, \qquad (1)$$

where E_{vac} — the energy of an electron that has left a solid-state structure and is in a vacuum near the surface of this structure; E_{F} — the Fermi energy of a solid-state structure. A number of papers address the calculation of the energy barrier for the electron to escape into vacuum and the calculation of the electron energy in vacuum, in close proximity to the surface [45–48]. The values of E_{F} and E_{vac} were calculated in this paper for the studied structures. The determination of the energy of an electron E_{vac} that left the structure and is in the immediate vicinity of the surface is an important point in such calculations. Let's focus on this point in a little more detail. The calculation of this energy is preceded by the calculation, within the framework of a self-consistent field, of the potential energy profile (or potential) $V_{\text{SCF}}(z)$ of an electron, as if „moving" from the quasi-2D-crystal lattice of a sample into vacuum, crossing atomic planes on its way. Here z means the direction along the axis perpendicular to the surface of the test sample. An averaging approach is used according to the following principle to determine the position of the central reference point of the potential $V_{\text{SCF}}(z)$ along the axis Z

$$V_{\text{SCF}}(z) = \frac{1}{d} \int_{z-d/2}^{z+d/2} V_{\text{SCF}}(z')dz', \qquad (2)$$

where d — the thickness of the quasi-2D-sample. The potential $V_{\text{SCF}}(z)$ is a solution of the electrostatic Poisson equation for a self-consistent field, which takes into account the contribution of all ionic skeletons of the atomic lattice. The potential $V_{\text{SCF}}(z)$ is averaged over all the supercell atoms of this plane within the limits of each atomic plane at a given coordinate z. The value of the interplane potential is averaged along the axis Z. Atomic oscillations are neglected because at normal temperature values they are negligibly small in amplitude.

3. Results

A graphene flake fragment containing 46 atoms and a nanotube fragment (16.0) with 64 atoms were used to construct an atomistic model of a 2D-graphene/nanotube film. This type of tube with a diameter of 1.2 nm was chosen as constituting one of the largest shares in the total mass of synthesized single-walled nanotubes. A fragment of a 2D-graphene/nanotube film is shown in Fig. 1, a, and a supercell — in Fig. 1, b, which also shows the distribution of electron charge density across atoms, calculated in within the framework of the Mulliken approach and represented in absolute values of the electron charge e. The supercell contains 110 atoms. The most noticeable charge redistribution is observed at the site of the covalent bond of the
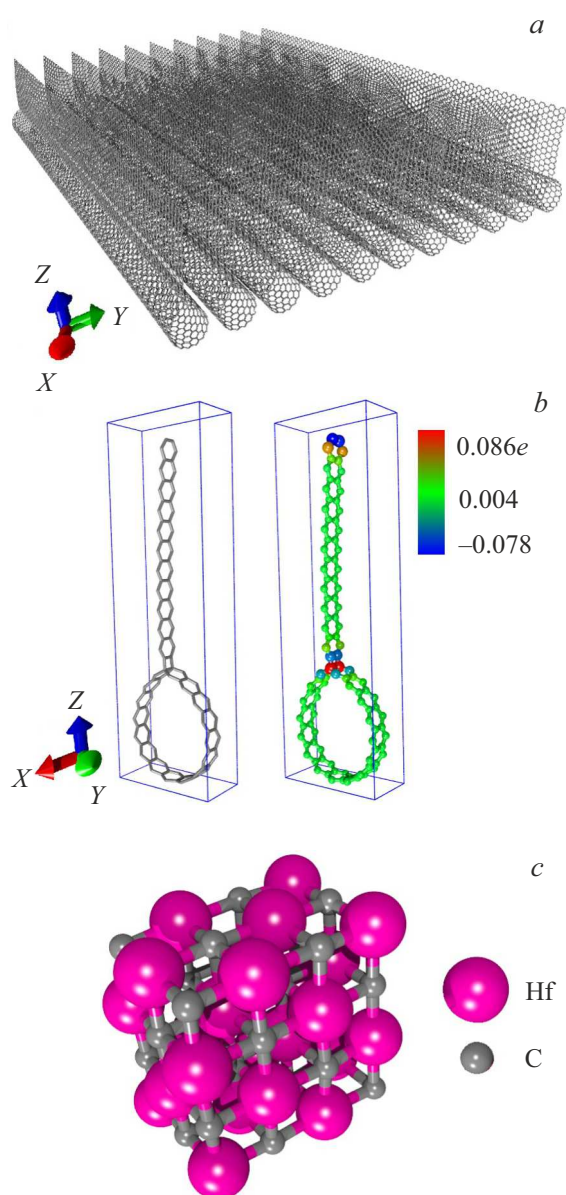
Figure 1. Atomistic models: a — 2D-graphene/nanotube film, b — its supercells and c — HfC nanoparticles.

nanotube with graphene and at the end of graphene. The edge atoms of the graphene sheet have an excess charge $-0.060e$, the atoms in the junction area with the tube — excess charge $-0.031e$. Thus, graphene carries an excessive negative charge $-0.021e$, and the tube — the corresponding positive charge, that is, when forming a hybrid structure, the charge from the tube partially flows to graphene. The atomic grid is distorted in the area of graphene-nanotube contact and graphene bending is observed, as well as tube narrowing in the plane YZ (Fig. 1, b), and its dimensions are 1.1×1.4 nm. The translation along the axis X is $L_x = 4.318$ Å, along the axis Y the translation step varied from 3.335 to 30 Å (the film in Fig. 1, a has a translation step along the axis Y $L_y = 15.9$ Å, which corresponds to

the distance between the tubes $R = 4.135$ Å). The minimum translation step along the axis Y corresponds to the optimal distance from the position of the Van der Waals interaction. The length of the graphene-tube interatomic bond in the junction area corresponds to the bond with C is in sp^3-hybridized state and is equal to 1.544 Å. The junction area is characterized by the presence of non-hexagonal elements, which makes this area active for the formation of new chemical bonds due to excessive electronic charge. A cubic cell with a spatial symmetry group $F\bar{m}3m$ and a crystal lattice step of 4.634 Å was used to construct an atomistic model of an HfC nanoparticle. A model of a subnanometer-sized nanoparticle was constructed, containing $1 \times 2 \times 2$ lattice cells in the directions $X \times Y \times Z$. As a result of optimization, the bond length Hf−Hf decreased compared to the 3D-variant and amounted to 4.345 Å, the bond length Hf−C is 2.239 Å. As a result, the nanoparticle sizes were $4.345 \times 7.510 \times 6.671$ Å. The type of nanoparticle is shown in Fig. 1, c. It contains 24 hafnium atoms and 24 carbon atoms. In fact, the HfC nanoparticle is a nanocrystalline, repeating the crystal cell of the 3D-crystal, since the symmetry does not change during optimization, but only the bond lengths change.

The electronic and emission characteristics calculated for 2D-graphene/nanotube film are presented in Table 1, where the values of Fermi energy, electron energy in vacuum at the surface and the work function at different distances R between the tubes are given (the distance is indicated between the walls of adjacent tubes).

The first results are given for a sufficiently large spacing step between the tubes, when the tubes are actually isolated from each other. Further, the distance decreases until the Van der Waals interaction occurs. The existence of an optimal distance between graphene/nanotube structures 4.135 Å was found when the work function is minimal and is 4.943 eV. The Fermi energy of the HfC nanoparticle is -3.712 eV.

Next, a 2D-graphene/nanotube film decorated with HfC nanoparticles was studied. Several different variants were considered, differing in the mass fraction of HfC nanoparticles. The first option with the maximum possible mass fraction of nanoparticles for this carbon frame was investigated from the standpoint of energy stability. The mass fraction of HfC nanoparticles was 53.6%. This variant corresponds to a structure whose super-cell is an extended

Table 1. Electronic and emission characteristics of quasi-2D-graphene/nanotube film

R, Å	L_y, Å	E_F, eV	E_{vac}, eV	Φ, eV
18.505	30.000	−4.928	0.089	5.016
4.535	16.400	−4.854	0.106	4.960
4.135	15.900	−4.829	0.114	4.943
3.735	15.400	−4.833	0.117	4.950
3.335	14.900	−4.835	0.119	4.954
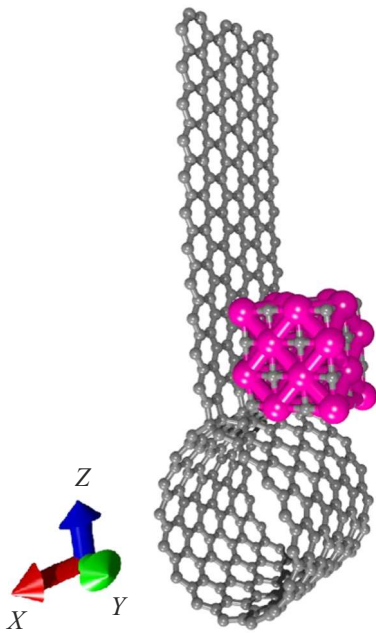
Figure 2. Expanded supercell of graphene/nanotube structure.

version of the carbon film cell shown in Fig. 1, *b*. The expanded supercell includes 3 initial cells, i.e. 330 carbon atoms. Its appearance is shown in Fig. 2. In this case, the translation step for X is $L_x = 12.954\,\text{Å}$, for Y — $L_y = 30\,\text{Å}$. The formation of such a composite structure is an exothermic process. The bond energy of a nanoparticle with a carbon frame is calculated as the difference between the total energy of the composite structure „carbon frame + nanoparticle HfC" (its super cells) and the energies of the initial components — the energy of the expanded carbon frame supercell (330 atoms) and the energy of the nanoparticle HfC $1 \times 2 \times 2$. In this case, the binding energy is equal to $-2132.72\,\text{eV}$, which indicates not only an exothermic process, but also the formation of a strong chemical bond. The distance between Hf atoms and C atoms of the carbon frame is in the range $2.26-2.29\,\text{Å}$. Fig. 3, *a* shows the calculated electron density of state profiles (DoS), given per unit of energy, for a carbon frame and for a frame decorated with HfC nanoparticles. The calculated partial densities of electronic states are also given (Fig. 3, *b*), which are introduced by carbon atoms and hafnium atoms.

The data in Fig. 3 show that the density of electronic states in the pure carbon frame decreases at the Fermi level, because the band structure is characterized at the gamma point by a small gap $\sim 0.02\,\text{eV}$. This gap in the DoS profile shifts to the left and narrows in case of decoration with nanoparticles, and a small peak of intensity appears at the Fermi level. Fig. 3, *b* clearly shows that carbon atoms make the main contribution to this small peak of intensity that has appeared. This is explained by a strong redistribution of the electron density in the „carbon frame + nanoparticle HfC" complex. In this complex, the nanoparticles flow from the

nanoparticle to the frame 0.26*e*, which changes the nature of the distribution of the density of electronic states in the energy range near the Fermi level. The contribution of various carbon and hafnium electrons to the formation of the DoS profile was studied. For carbon atoms these are *p*-electrons of the second electron layer, for hafnium atoms these are *d*-electrons of the fifth layer.

Then the distance between the tubes R decreased while maintaining the mass fraction of HfC nanoparticles 53.6 and 36.6%. Table 2 shows the calculated values of the Fermi energy, the electron energy in vacuum at the surface and the work function for the same translational distances L_y, which were presented in Table 1.

As can be seen from the data in the table, the behavior of the work function with a change in the parameter L_y does not coincide with the results of studies obtained for pure quasi-2D-graphene/nanotube films. The minimum value of the work function falls on the inter-tube distance of $18.505\,\text{Å}$, that is, on the value of $L_y = 30\,\text{Å}$. For this reason the studies of the impact of the spacing step of graphene/nanotube structures decorated with HfC nanoparticles on the work function were continued. Fig. 4, *a* shows the change of the work function with a distance R at the values of the mass fraction of HfC 53.6 and 36.7%. Calculation points and approximating curves are presented. A fragment of a film with a mass fraction of 36.7% at a step along the axis Y equal to 2.5 nm is shown in the insert (at this distance step, the value of the work function from the interval of minimum values is observed). Analysis of the data in Fig. 4, *a* shows that there is an optimal distance interval between tubes with graphene sheets, which gives the lowest values of the output operation. The interval of these distances for two different values of the mass fraction of HfC nanoparticles is the same — $2.0-2.8$ nm. Approximating curves are quadratic functions. This is a function $Y = 0.668 - 0.946X + 0.182X^2$ for the case of mass fraction 53.6% or $Y = 6.246 - 1.425X + 0.282X^2$ for the case of mass fraction 36.6%.

Table 2. Electronic and emission characteristics of quasi-2D-graphene/nanotube film decorated with HfC nanoparticles with different mass fraction

R, Å	L_y, Å	E_F, eV	E_{vac}, eV	Φ, eV
Mass fraction 53.6%				
18.505	30.000	-4.387	0.082	4.469
4.535	16.400	-4.525	0.100	4.625
4.135	15.900	-4.531	0.102	4.633
3.735	15.400	-4.538	0.103	4.641
3.335	14.900	-4.545	0.104	4.648
Mass fraction 36.7%				
18.505	30.000	-4.432	0.073	4.505
4.535	16.400	-4.522	0.099	4.621
4.135	15.900	-4.574	0.130	4.704
3.735	15.400	-4.602	0.140	4.742
3.335	14.900	-4.625	0.148	4.773
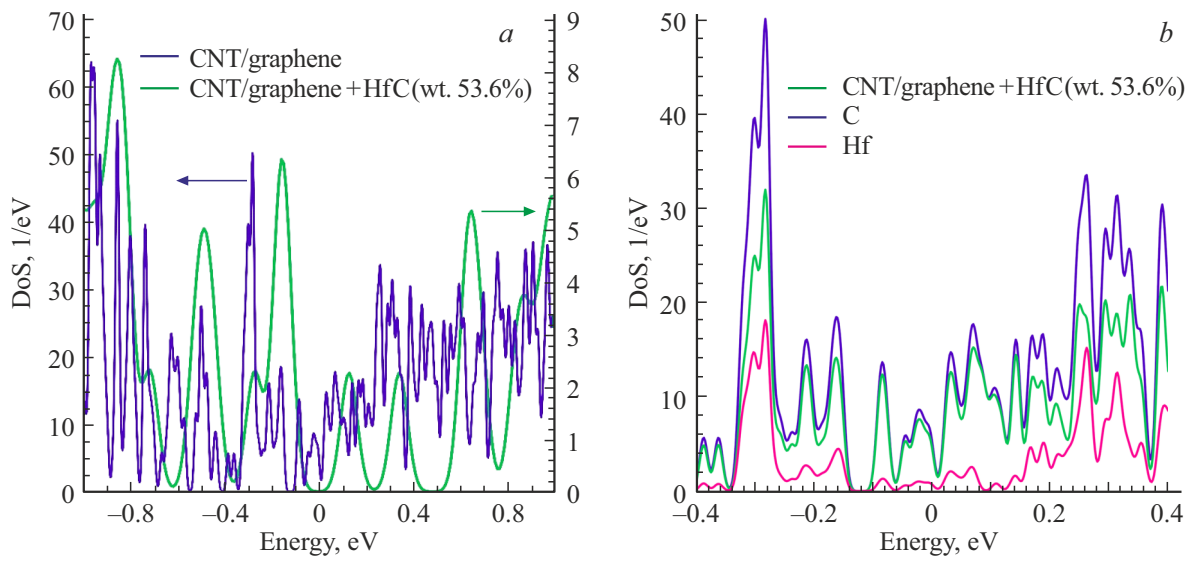
Figure 3. Graphene/nanotube structure with translational step along the axis Y 30 Å: a — density of electronic states of pure carbon frame and HfC functionalized by nanoparticles; b — partial densities of electronic states. The Fermi level is at zero.
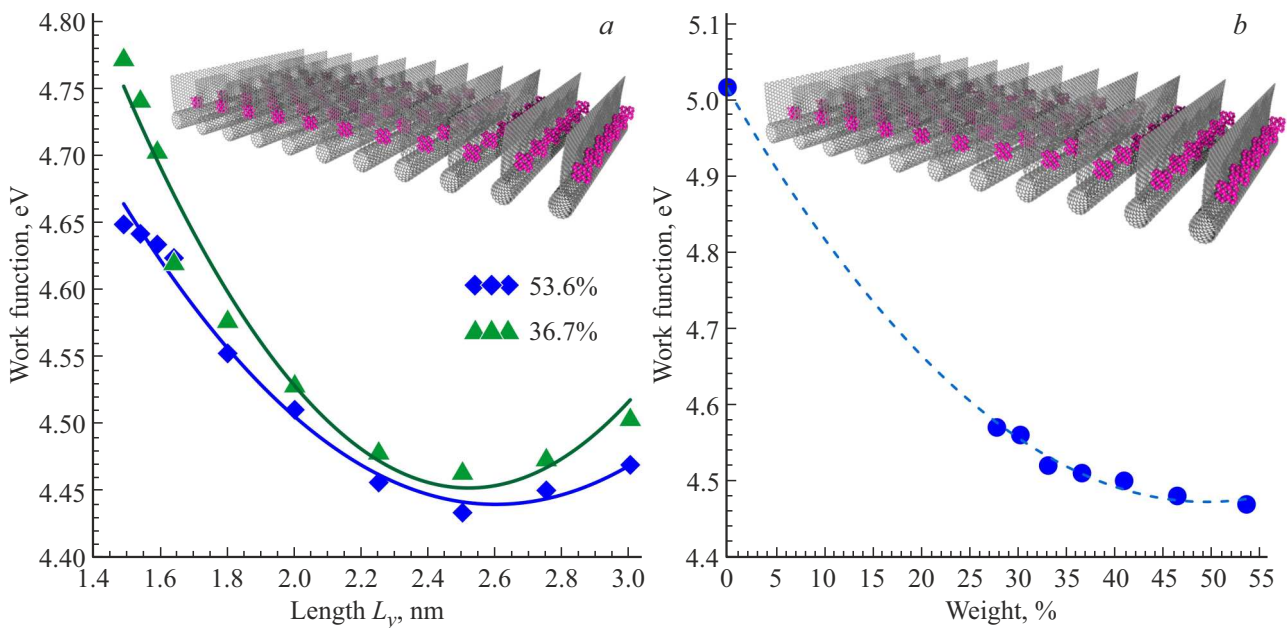
Figure 4. Change of the work function a — depending on the distance between graphene/nanotube structures (at a mass fraction of HfC 53.6 and 36.7%) and b — depending on the mass fraction of HfC at the periodic step $L_y = 2.5$ nm.

Next, the effect of the mass fraction of HfC nanoparticles on the film output at the optimal translational step along the axis Y from the set interval 2.0−2.8 nm was investigated. The translational step $L_y = 2.5$ nm (the middle of the interval) was selected. That is, with a fixed step between the tubes, the mass fraction of nanoparticles consistently decreased from 53.6 to 27.8%. The mass fraction of HfC decreased by increasing the carbon frame by 110 atoms. The carbon frame contains 990 atoms with a mass fraction of 27.8%. Calculations *ab initio* are resource-intensive and require a lot of time, so it was not possible to further

increase the carbon frame and further reduce the mass fraction, at least at present. Graphs of changes in the output operation are shown in Fig. 4, b. The decrease in the output operation occurs non-linearly according to the quadratic law, as it is established from the data obtained by us. The function describing the reduction of the output has the form $Y = 5.016 - 0.025X + 0.0002X^2$. It can be seen that the output work decreases rapidly with an increase in the mass fraction of HfC to 30%, but already at 40% the decrease reaches saturation, and a further increase in the mass fraction affects the output work less and less.

4. Conclusion

The regularities of the impact of hafnium carbide HfC nanoparticles on the electronic and emission properties of quasi-2D-graphene/nanotube films were found. It was found that two key factors impact the decrease of the work function — the distance between graphene/nanotube structures in the film and the mass fraction of HfC nanoparticles. Taken together, these two points make it possible to achieve a reduction in the output by more than 10%. The new knowledge obtained is important for evaluating the autoemission properties of similar carbon quasi-2D-nanostructures that can be used as a blade autoemission cathode.

Funding

Conflict of interest

The authors declare that they have no conflict of interest.

References

[1] A.G. Rinzler, J.H. Hafner, P. Nikolaev, P. Nordlander, D.T. Colbert, R.E. Smalley, L. Lou, S.G. Kim, D. Tomanek. Sci. **269**, 5230, 1550 (1995).

[2] W.A. De Heer, A. Châtelain, D. Ugarte. Sci. **270**, *5239*, 1179 (1995).

[3] L.A. Chernozatonskii, Y.V. Gulyaev, Z.Ja. Kosakovskaja, N.I. Sinitsyn, G.V. Torgashov, Yu.F. Zakharchenko, V.P. Val'chuk. Chem. Phys. Lett. **233**, *1−2*, 63 (1995).

[4] Yu.V. Gulyaev, N.I. Sinitsyn, G.V. Torgashov, Sh.T. Mevlyut, A.I. Zhbanov, Yu.F. Zakharchenko, Z.Ya. Kosakovskaya, L.A. Chernozatonskii, O.E. Glukhova, I.G. Torgashov. J. Vac. Sci. Technol. B **15**, *2*, 422 (1997).

[5] A.V. Eletskii. Phys. Usp. **53**, *9*, 863 (2010).

[6] E.D. Eidelman, A.V. Arkhipov. Phys. Usp. **63**, *7*, 648 (2020).

[7] N.R. Sadykov, S.E. Zholnirov, I.A. Pilipenko. Tech. Phys. **66**, *9*, 1032 (2021).

[8] N. Shimoi, Y. Sato, K. Tohji. ACS Appl. Electron. Mater. **1**, *2*, 163 (2019).

[9] C. Huo, F. Liang, A.-B. Sun. High Voltage **5**, *4*, 409 (2020).

[10] X. Liu, Y. Li, J. Xiao, J. Zhao, C. Li, Z. Li. J. Mater. Chem. C **11**, *7*, 2505 (2023).

[11] R.K. Yafarov. Radiotekhnika i elektronika a **64**, *12*, 1238 (2019). (in Russian).

[12] M.V. Davidovich, R.K. Yafarov. Tech. Phys. **63**, *2*, 274 (2018).

[13] N.A. Bushuev, O.E. Glukhova, Yu.A. Grigor'ev, D.V. Ivanov, A.S. Kolesnikova, A.A. Nikolaev, P.D. Shalaev, V.I. Shesterkin. Tech. Phys. **61**, *2*, 290 (2016).

[14] M. Komlenok, N. Kurochitsky, P. Pivovarov, M. Rybin, E. Obraztsova. Nanomater. **12**, *11*, 1934 (2022).

[15] Y. Gao, S. Okada. Nano Express **3**, *3*, 034001 (2022).

[16] J. Gong, P. Yang. RSC Adv. **4**, *38*, 19622 (2014).

[17] J. Gong, H. Yang, P. Yang. Composites B **75**, 250 (2015).

[18] D.D. Nguyen, R.N. Tiwari, Y. Matsuoka, G. Hashimoto, E. Rokuta, Y.Z. Chen, Y.L. Chueh, M. Yoshimura. ACS Appl. Mater. Interfaces **6**, *12*, 9071 (2014).

[19] D.D. Nguyen, N.H. Tai, S.Y. Chen, Y.L. Chueh. Nanoscale **4**, *2*, 632 (2012).

[20] M. Song, P. Xu, Y. Song, X. Wang, Z. Li, X. Shang, H. Wu, P. Zhao, M. Wang. AIP Advances **5**, *9*, 097130 (2015).

[21] S. Riyajuddin, S. Kumar, K. Soni, S.P. Gaur, D. Badhwar, K. Ghosh. Nanotechnol. **30**, *38*, 385702 (2019).

[22] L. Chen, H. He, H. Yu, Y. Cao, D. Lei, Q. Menggen, C. Wu, L. Hu. J. Alloys. Compd. **610**, 659 (2014).

[23] X. Hong, W. Shi, H. Zheng, D. Liang. Vacuum **169**, *7*, 108917 (2019).

[24] R.T. Lv, E. Cruz-Silva, M. Terrones. ACS Nano **8**, *5*, 4061 (2014).

[25] W. Du, Z. Ahmed, Q. Wang, C. Yu, Z. Feng, G. Li, M. Zhang, C. Zhou, R. Senegor, C.Y. Yang. 2D Mater. **6**, *4*, 042005 (2019).

[26] S. Pyo, Y. Eun, J. Sim, K. Kim, J. Choi. Micro. Nano Syst. Lett. **10**, 9 (2022).

[27] L.A. Chernozatonskii, E.F. Sheka, A.A. Artyukh. JETP Lett. **89**, *7*, 352 (2009).

[28] A.A. Artyukh, L.A. Chernozatonskii, P.B. Sorokin. Physica Status Solidi B **247**, *11−12*, 2927 (2010).

[29] B.Yu. Valeev, A.N. Toksumakov, D.G. Kvashnin, L.A. Chernozatonskii. JETP Lett. **115**, *2*, 93 (2022).

[30] J. Srivastava, A. Gaur. J. Chem. Phys. **155**, *24*, 244104 (2021).

[31] A.B. Felix, M. Pacheco, P. Orellana, A. Latgé. Nanomater. **12**, *19*, 3475 (2022).

[32] O.E. Glukhova, I.S. Nefedov, A.S. Shalin, M.M. Slepchenkov. Beilstein J. Nanotechnol. **9**, 1321 (2018).

[33] L. Wei, L. Zhang. Nanomater. **12**, *8*, 1361 (2022).

[34] S. Tang, J. Tang, T.W. Chiu, J. Uzuhashi, D.-M. Tang, T. Ohkubo, M. Mitome, F. Uesugi, M. Takeguchi, L.-C. Qin. Nanoscale **12**, *32*, 16770 (2020).

[35] T.W. Chiu, J. Tang, S. Tang, J. Yuan, L.C. Qin. Physica Status Solidi A **217**, *10*, 2000007 (2020).

[36] A. Nisar, L. Lou, B. Boesl, A. Agarwal. Carbon **205**, 573 (2023).

[37] S. Tian, L. Zhou, Z. Liang, Y. Yang, Y. Wang, X. Qiang, S. Huang, H. Li, S. Feng, Z. Qian, Y. Zhang. Carbon **161**, 331 (2020).

[38] H. Liang, L. Fang, S. Guan, F. Peng, Z. Zhang, H. Chen, W. Zhang, C. Lu. Inorg. Chem. **60**, *2*, 515 (2021).

[39] J.M. Soler, E. Artacho, J.D. Gale, A. García, J. Junquera, P. Ordejón, D. Sánchez-Portal. J. Phys.: Condens. Matter **14**, *11*, 2745 (2002).

[40] J.P. Perdew, J.A. Chevary, S.H. Vosko, K.A. Jackson, M.R. Pederson, D.J. Singh, C. Fiolhais. Phys. Rev. B **46**, *11*, 6671 (1992).

[41] H.J. Monkhorst, J.D. Pack. Phys. Rev. B **13**, *12*, 5188 (1976).

[42] P. Pulay. Chem. Phys. Lett. **73**, *2*, 393 (1980).

[43] R.S. Mulliken. J. Chem. Phys. **23**, *10*, 1833 (1955).

[44] S. Grimme. J. Comput. Chem. **27**, *15*, 1787 (2006).

[45] R. Tran, X.G. Li, J.H. Montoya, D. Winston, K.A. Persson, S.P. Ong. Surf. Sci. **687**, 48 (2019).

[46] J. Wang, S.-Q. Wang. Surf. Sci. **630**, 216 (2014).

[47] D.-P. Ji, Q. Zhu, S.-Q. Wang. Surf. Sci. **651**, 137 (2016).

[48] S.D. Waele, K. Lejaeghere, M. Sluydts, S. Cottenier. Phys. Rev. B **94**, *23*, 235418 (2016).

[49] H.L. Skriver, N.M. Rosengaard. Phys. Rev. B **46**, *11*, 7157 (1992).

Translated by A.Akhtyamov